ISSN-e: 1690-8791

# REAL-TIME MONITORING OF RESIDENCE TIME IN A CONTINUOUS REACTOR USING TRACERS AND MATLAB

ALEXANDER BALZA
alza.alexander@correo.unimet.edu.ve
Universidad Metropolitana de Caracas, (Venezuela)
ANDREINA IDLER
andreina.idler@correo.unimet.edu.ve
Universidad Metropolitana de Caracas, (Venezuela)
AURIMAR RASQUIN
xxxxx@correo.unimet.edu.ve
Universidad Metropolitana de Caracas, (Venezuela)
NATALIA FERNÁNDEZ
natalia.fernandez@correo.unimet.edu.ve
Universidad Metropolitana de Caracas, (Venezuela)
NICOLE MORENO
nicole.moreno@correo.unimet.edu.ve
Universidad Metropolitana de Caracas, (Venezuela)
RICARDO ÁVILA
ricardo.avila@correo.unimet.edu.ve
Universidad Metropolitana de Caracas, (Venezuela)
ROSA MONTES DE OCA
montesdeoca.rosa@correo.unimet.edu.ve
Universidad Metropolitana de Caracas, (Venezuela)
SOPHIA FUNG
sophia.fung@correo.unimet.edu.ve
Universidad Metropolitana de Caracas, (Venezuela)
MIGUEL PÉREZ
mperez@unimet.edu.ve
Universidad Metropolitana de Caracas, (Venezuela)

## Abstract:

Determining residence time (RTD) is essential for optimizing chemical processes, as it influences reagent conversion, product selectivity, and overall reactor efficiency. This study focuses on characterizing RTD distribution in a laboratory-scale vertical piston flow reactor using a dye

RECEIVED: 09-07-2025 / ACCEPTED: 13-09-2025 / PUBLISHED: 22-12-2025

**How to quote:** Balza et al. (2025). Real-time monitoring of residence time in a continuous reactor using tracers and MATLAB. *Cuadernos Unimetanos*, 42, 25 - 48. https://doi.org/10.58479/cu.2025.191

tracer and a real-time data acquisition system. An experimental system was implemented that includes a peristaltic pump, an LDR light sensor, an Arduino UNO, and an application developed in MATLAB App Designer for data collection and analysis. The results indicate that increasing the flow rate reduces the average residence time, and the use of the Weibull distribution to model the non-ideal behavior of the reactor was validated. This work not only contributes to the characterization of non-ideal reactors, but also provides an educational platform that allows students to replicate the experiment and analyze data in real time, highlighting the usefulness of modern tools in teaching key concepts in chemical engineering. This study is aligned with SDGs 4 (Quality Education), 9 (Industry, Innovation, and Infrastructure), and 12 (Responsible Consumption and Production).

Keywords: piston flow reactor, residence time distribution (RTD), Weibull distribution, dye tracer, data acquisition, quality education, responsible production and consumption, innovation.

## Sustainable Development Goal(s) (SDG) to which the research work is directed

### 4- QUALITY EDUCATION

Description
Ensure inclusive and equitable quality education and promote lifelong learning opportunities for all.

Relationship
Provide an innovative and accessible educational platform for experimental teaching in chemical engineering.

Direct Objective

### 9- INDUSTRY, INNOVATION, AND INFRASTRUCTURE

Description
Build resilient infrastructure, promote inclusive and sustainable industrialization, and foster innovation.

Relationship
Through the integration of low-cost technologies (Arduino, optical sensors, and MATLAB) for real-time monitoring of industrial processes.

Direct Objective

### 12- RESPONSIBLE PRODUCTION AND CONSUMPTION

Dscription
Ensure sustainable consumption and production patterns.

Relationship
Promote efficient and replicable methodologies that optimize resources in teaching laboratories and foster sustainability in the training of future engineers.

Direct Objective

ISSN-e: 1690-8791

## INDEX

## Introduction

Chemical reactors are fundamental equipment in chemical engineering, designed to maximize reagent conversion and product selectivity while minimizing operating costs. Among continuous flow reactors, the piston flow reactor (PFR) stands out for its unidirectional axial flow, which ideally does not mix in the direction of flow. However, in practice, actual reactors often deviate from this ideal behavior due to phenomena such as axial dispersion and the formation of stagnant zones, which affect residence time distribution (RTD) and, consequently, process efficiency. Experimental determination of RTD is crucial for understanding and optimizing these systems, especially in educational applications where students must learn to relate theory to practice.

This work presents an experimental study to characterize the RTD in a laboratory-scale RFP, using a dye tracer and real-time data acquisition tools. This approach not only allows for the validation of theoretical models, but also demonstrates the application of modern technologies in chemical engineering education, thus contributing to the Sustainable Development Goals (SDGs) 4 ( education) and 9 (Industry, Innovation, and Infrastructure).

The experimental design and data acquisition system developed in this study offer a valuable tool for teaching chemical engineering. Students can replicate the experiment using accessible materials, such as a peristaltic pump, LDR light sensors, and a data processing platform based on Arduino and MATLAB. This setup allows them to understand in detail the determination of the RTD, the influence of flow rate on residence time, and the application of mathematical models such as the Weibull distribution to describe the behavior of the system.

In addition, this approach facilitates the learning of key competencies in instrumentation and data analysis, promoting the development of practical skills in sensor handling, data acquisition, and mathematical modeling. The ability to visualize and analyze the system's response to operational changes in real time reinforces the connection between theory and practice, preparing students to face real-world problems in reactor design and optimization. Therefore, this study not only contributes to the analysis of RTD in non-ideal reactors, but also serves as an educational platform for teaching fundamental principles of chemical kinetics, fluid dynamics, and process control, consolidating the use of active methodologies in the training of chemical engineers.

This work can be used as a valuable educational tool in various areas of knowledge. Students can replicate the experiment described in this article using the detailed materials and procedures, allowing them to observe the results firsthand. In addition, the analysis of the data obtained fosters understanding of statistical methods and the interpretation of results, promoting discussions about their validity. Additional projects can be proposed to expand the scope of this work, encouraging students to investigate beyond the original experiment. This not only improves their understanding of the subject, but also develops research and critical thinking skills.

A chemical reactor is a piece of equipment designed to carry out a chemical reaction in a controlled manner, with the aim of maximizing the conversion of reactants and the selectivity of the products, while minimizing operating costs [1]. Inside, the reactants are introduced under specific temperature and pressure conditions in order to facilitate their transformation into desired products through physical and chemical processes. [2]

In chemical engineering, reactors are mainly classified according to fluid flow, distinguishing between continuous flow reactors and batch reactors. Continuous flow reactors are those in which reactants are fed and products are removed continuously throughout the process. One of the most representative models of this type of reactor is the piston flow reactor (PFR), which operates with a unidirectional axial flow through a tube, without significant mixing in the direction of flow, a configuration that results in a concentration profile that varies throughout the reactor [3].

### *Flow models*

The flow of fluids in a reactor is a fundamental aspect that determines the behavior and efficiency of a chemical reaction process [4]. In ideal models, uniform and predictable fluid behavior within the reactor is assumed. However, in practice, reactors often behave non-ideally due to a number of factors that affect fluid distribution and transport, which can significantly alter the efficiency of the reaction [5].

Wall effects refer to the influence of reactor surfaces on fluid flow. These effects can cause the fluid to slow down near the walls, altering the velocity and distribution of concentrations throughout the reactor [6][7].

In addition, proximity to the walls can induce fluid accumulation phenomena, which can favor the formation of zones with higher concentrations of products or reactants, affecting the homogeneity of the process [8].

Axial dispersion, on the other hand, describes the tendency of the fluid to diffuse forward or backward along the reactor due to variations in fluid velocity [9]. This phenomenon causes less predictable behavior in terms of the distribution of reagent and product concentrations, reducing the efficiency of the reaction by allowing some portions of the fluid to react more slowly than others [10].

These effects are common characteristics in real reactors, and as reactors are scaled up or designed with more complex geometries, non-ideal phenomena become more pronounced, necessitating the use of advanced models to describe fluid flow and predict reaction behavior under real conditions [4]. Therefore, understanding and mitigating these effects is crucial to improving the efficiency and safety of industrial chemical reaction processes.

### *Residence time*

Knowing the average time that particles remain inside a reactor is essential to understanding the behavior of reactants and products throughout the reaction process, as this time directly influences the conversion of reactants, the formation of products, and the overall efficiency of the process. Thus, the concept of residence time emerges to quantify the average time that particles remain inside a reactor.

In non-ideal reactors, this time is not homogeneous, which can lead to non-uniform time distributions due to flow phenomena, meaning that some portions of the fluid may pass through the reactor more quickly than others, affecting conversion efficiency and product selectivity. In this context, the residence time distribution, known as the residence time distribution function $E(t)$ , represents the fraction of fluid that leaves the reactor after remaining there for a specific time.

$$E(t) = \frac{C(t)}{\int_0^{\infty} C(t)\,dt} \qquad \mathbf{(1)}$$

Where:

$E(t)$: Residence time distribution function.

$C(t)$: Tracer concentration at the reactor outlet at time t.

$\int_0^{\infty} C(t)dt$: Area under the concentration versus time curve, which normalizes $E(t)$ so that its total integral is 1.

The simplest and most direct experimental methods for determining the residence time distribution curve use a non-reactive tracer. In this case, a substance that does not participate in the chemical reaction is introduced, and its concentration can be tracked over time to determine how it is distributed in the reactor. Among the most common methods are pulse experiments, which consist of suddenly injecting a small amount of tracer into the system and observing how it is distributed throughout the reactor [3].

In non-ideal reactors, this distribution is extended, and its shape depends on the reactor geometry and flow characteristics, so the resulting residence time distribution curve does not follow a symmetric distribution. To model these asymmetric distributions, more flexible functions are used, such as the Weibull distribution, which is widely used in non-ideal systems. The probability density function of the Weibull distribution is defined by:

$$E(t)_{Weibull} = a \cdot \left(\frac{t}{b}\right)^{c-1} \cdot e^{-\left(\frac{t}{b}\right)^{c}}, t \geq 0 \quad \textbf{(2)}$$

So that:

$a$: Normalization parameter, which adjusts the total magnitude of the curve.

$b$: Time scale parameter, related to the average residence time.

$c$: Shape parameter, which defines the asymmetry of the distribution.

In practice, controlling the residence time is necessary to optimize the reactor's operating conditions, ensuring that the reactants have enough time to achieve the desired conversion without the process becoming unnecessarily long or costly. In addition, the residence time influences the scale of the reactor, since, for large production volumes, it is necessary to adjust the flow rate and volume of the reactor to maintain adequate residence times for the complete or desired conversion of the reactants [11].

## Research objectives

- Select the most suitable tracer, evaluating various substances based on their compatibility with the experimental setup, to enable rapid measurement of residence time without interruptions in the continuous flow.
- Establish the relationship between the applied voltage and the flow rate delivered by a peristaltic dosing pump, through experimental measurements, to achieve precise control of the water flow.
- Program the real-time data acquisition of the LDR light sensor using an Arduino UNO, through a suitable experimental setup.
- Construct a calibration curve, using solutions of known input concentrations, to obtain the correlation between the photoresistor sensor readings and the output concentrations of the tracer.

- Develop an application in MATLAB App Designer to obtain the residence time distribution curve, in order to facilitate real-time analysis in a continuous reactor flow.
- Analyze the dynamic response of the reactor by introducing the tracer at different flow rates and concentrations to observe variations in residence time.

## Experimental design

For the development of the project, a 50 mL burette was selected to allow a constant flow of solvent and simulate a continuous reactor. Red food coloring was used as a tracer due to its low cost and stability. This dye was diluted in filtered water to prevent damage to the hoses and pump.

Two requirements were established for tracer detection: an adequate sampling frequency and real-time measurement. A detector of changes in luminosity was designed with an LED and an LDR sensor, inexpensive and versatile devices that allowed real-time data to be obtained on changes in solvent coloration [12].

### *Phase 1.* Calibration of the water distribution system

To ensure controlled water flow, a 24-volt Grothen peristaltic dosing pump was used, along with serum hoses with an internal diameter of 2 mm. The electrical system was powered by a Trygon Electronics power supply, and the applied voltage was monitored using an AstroAI WH5000A voltmeter. The voltages were varied within the pump's operating range (16 to 24 V), and the time required to fill a 40 mL volume in the burette was recorded. The volumetric flow rate was determined using the following equation:

$$Q = \frac{V}{t} \qquad (3)$$

where $V$ is the known volume in milliliters and $t$ is the time measured in seconds. For each voltage value, three independent flow measurements were taken, and the average of the values obtained was calculated. In this way, a linear fit equation was obtained that describes the flow delivered as a function of the applied voltage. This can be seen in Figure I.

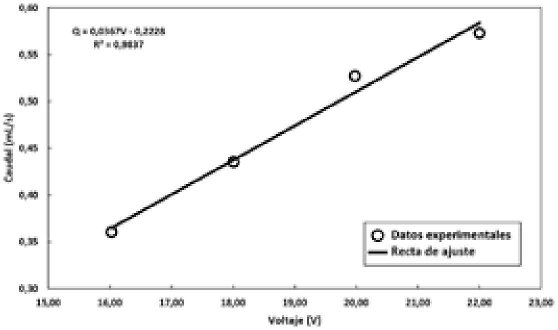

FIGURE I

Calibration curve for the Grothen peristaltic pump.

*Phase 2.* Design of a system for detecting changes in light intensity

An effective method for monitoring tracer concentration in real time is to use optical sensors based on the detection of changes in light intensity, which can be related to the presence and concentration of the tracer in the flow [14]. This idea is based on the interaction between light and matter, where the absorption, scattering, and transmission of light depend on the optical properties of the medium through which it passes [14].

In other words, red bodies, such as the dye used, mainly absorb wavelengths between 490 and 580 nm, corresponding to green, their complementary color. This interaction generates greater absorption of green light and, therefore, greater attenuation of the light reflected or transmitted to the sensor. This effect is explained by Lambert-Beer's law, which relates the amount of light absorbed and the amount of light transmitted in a species as a function of its concentration and wavelength. This phenomenon increases the sensitivity of the system and improves the accuracy of the dye concentration measurement by reducing interference from other components that may absorb light at other wavelengths. This variation in light intensity is what allows for accurate detection of changes in the concentration of fluids passing through the burette [15].

Regarding the LDR sensor, it is relevant to mention the phenomenon of the photoelectric effect, which refers to the emission of electrons when electromagnetic radiation strikes a material. Thanks to this effect, as the amount of light received by the LDR increases, its resistance decreases, allowing more current to flow to the Arduino. Consequently, the absorption of light by the LDR causes a change in the electrical conductivity of the material, allowing variations in light intensity to be detected [16].

The LED and encapsulated sensor system (Figure II) was connected to an Arduino microcontroller, which recorded data at regular intervals every tenth of a second (Figure III).

FIGURE II

Design of the light change detection system
(PLA piece, white LED, and photoresistor sensor)

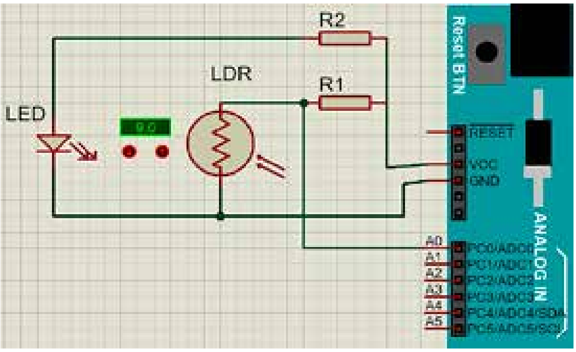

FIGURE III

Arduino wiring
Note: the diagram was created using Protheus software

Given that the data obtained from the Arduino correspond to sensor readings and not to the tracer output concentrations, a calibration curve was created for the light change detection system. This procedure consisted of introducing each prepared solution, with concentrations established in Table I, into the reactor and, with the sensor previously activated, collecting the readings at the respective concentrations.

Figure IV shows the final experimental setup of the reactor.

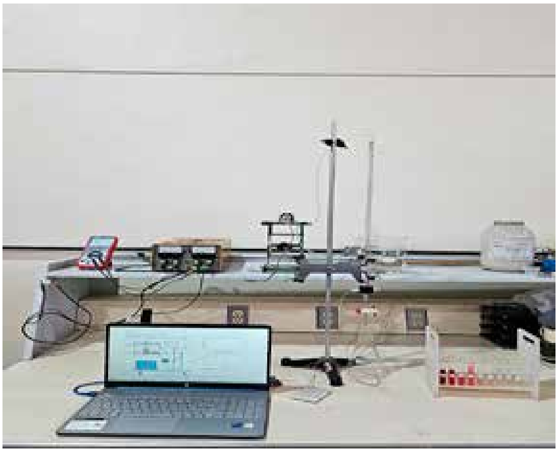

FIGURE IV

Experimental setup of the reactor

*Phase 3.* Standardization of tracer solutions

Since the data obtained from the Arduino correspond to sensor readings and not directly to the dye concentrations in the effluent, a calibration curve was developed to correlate these readings with the dye output concentrations. This procedure consisted of introducing prepared solutions with known concentrations, as shown in Table I, into the reactor.

TABLE I

Concentrations of food coloring solutions diluted in water

| Solution | A | B | C | D | E | F | G | H | I |
|---|---|---|---|---|---|---|---|---|---|
| Concentration (mg/mL) | 1.1109 | 0.3703 | 0.1230 | 0.0823 | 0.0411 | 0.0137 | 0.0046 | 0.0015 | 0.0005 |

The serial dilution method was used to prepare the different concentrations. Starting with a 10% m/v (mg/mL) stock solution

The dilution factor was calculated using the following formula:

$$F = \frac{Vp}{Vf+Vp} = 0.333 \qquad (4)$$

where$Vp$ is the flow volume, which was kept fixed at 5 mL, and$Vf$ is the solvent volume, which was kept at 10 mL.

Based on the dilution factor and knowing the concentration of the stock solution, the concentrations of the successive dilutions were calculated using the following equation:

$$C_{i+1} = C_i \cdot F \qquad (5)$$

where$Ci$ is the previous concentration and$F$ is the dilution factor.

The calibration curve obtained from the experimental data is shown below.

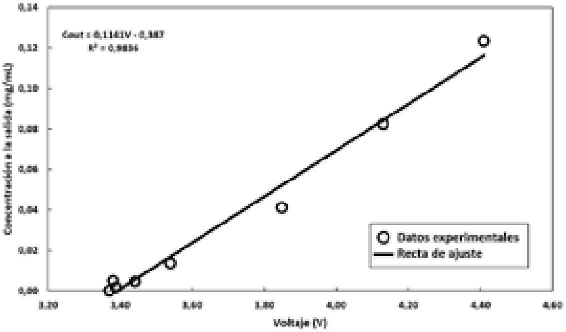

FIGURE V

Calibration curve of the dye

## *Phase 4.* Development of a MATLAB App Designer application to determine the residence time of the tracer

An Arduino microcontroller with an LDR sensor was used to measure variations in light intensity, which correspond to the concentration of the tracer in the system. A sampling system was programmed at 0.1-second intervals to ensure accuracy in data collection. The measurements were stored in a dynamic array that automatically expanded with new data, allowing the evolution of the tracer concentration to be recorded without interruption.

The application developed had the ability to graphically represent the data in real time, generating a curve that showed the variation in light intensity as a function of tracer concentration. This allowed for immediate monitoring of the system's behavior. After collecting the data, it was fitted to a Weibull mathematical model, known for describing distributions with long, asymmetric tails, common in continuous reactor flow systems. This fit provided an accurate representation of the temporal distribution of the tracer. Finally, spatial time was considered a key variable for analyzing the residence time of the tracer, related to the geometry and flow characteristics within the reactor.

*Phase 5.* Start of the experiment. Tracer injection.

First, a computer was connected to the Arduino to receive the data perceived by the sensor; the pump was turned on and the reactor was stabilized until a steady state of the system was achieved. Subsequently, an aliquot of this volume of the solution at the chosen concentration was measured with a 1 mL volumetric pipette; this sample was added through the upper part of the reactor to the burette system at the same time as recording began in the application developed in MATLAB for data collection and processing.

*Phase 6.* Repetition of the experiment.

To verify the behavior of the reactor, it was decided to initially conduct the experiment by fixing the flow rate and varying the tracer concentrations. Subsequently, the concentration was fixed and the flow rate supplied to the burette was varied. In order to compare the results obtained, the procedure described in the previous step was repeated, starting the experiment and injecting the tracer, using the previously established parameters, performing each experiment in triplicate. Table II shows the parameters of the compared variables:

TABLE II

Definition of the parameters studied

| Concentrations (mg/mL) used with a fixed flow rate of 0.36 mL/s. | Flow values (mL/s) used at a fixed concentration of 1.1109 mg/mL |
|---|---|
| 1.1109 | 0.36 |
| 0.3703 | 0.57 |

## Results and discussions

Figure VI shows the triplicate results of the experiment with a defined flow rate of 0.36 mL/s and a concentration of 1.1109 mg/mL.

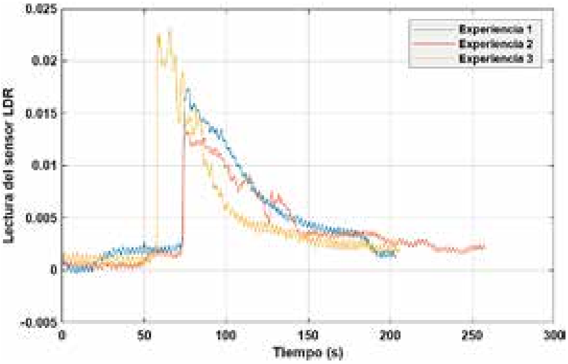

FIGURE VI

Curve of the raw sensor reading with a flow rate of 0.36 mL/s and a tracer concentration of 1.1109 mg/mL in real time.

Figure VII shows the results obtained with the Weibull distribution for the residence time with a defined flow rate at a voltage of 0.36 mL/s and a concentration of 1.1109 mg/mL.

.

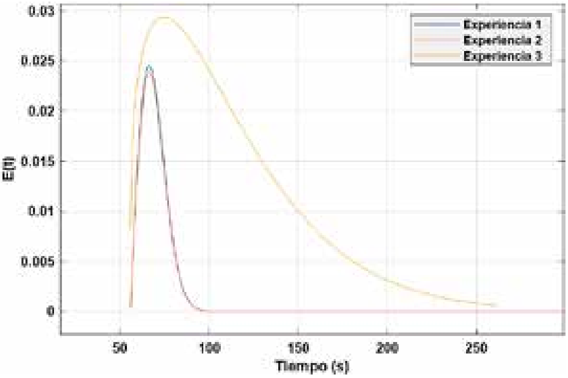

FIGURE VII

Weibull distribution for residence time with a flow rate of 0.36 mL/s and a tracer concentration of 1.1109 mg/mL.

Figure VIII illustrates the triplicate results of the experiment whose defined parameters were a flow rate of 0.57 mL/s and a tracer concentration of 1.1109 mg/mL.

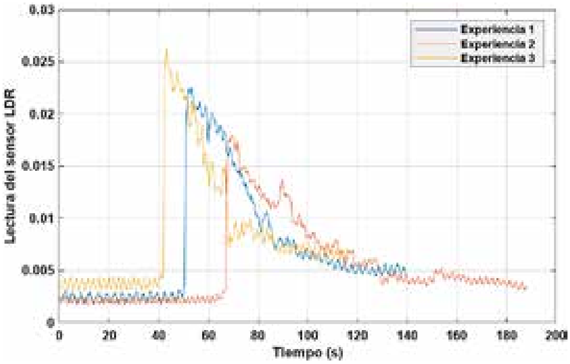

FIGURE VIII

Curve of the raw sensor reading with a flow rate of 0.57 mL/s and a tracer concentration of 1.1109 mg/mL in real time.

Figure IX shows the results obtained by applying the Weibull distribution for the residence time, with a flow rate set at a voltage of 0.57 mL/s and a concentration of 1.1109 mg/mL.

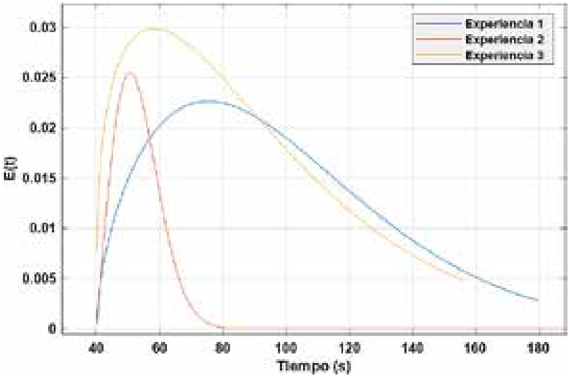

FIGURE IX

Weibull distribution for residence time with a flow rate of 0.57 mL/s and a tracer concentration of 1.1109 mg/mL.

For the results of the three experiments carried out with a flow rate set at 0.36 mL/s and an initial tracer concentration of 0.3703 mg/mL, the graph shown in Figure X was developed.

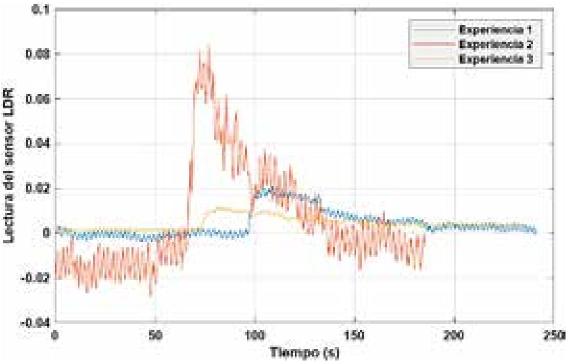

FIGURE X

Curve of the raw sensor reading with a flow rate of 0.36 mL/s and a tracer concentration of 0.3703 mg/mL in real time.

The Weibull distribution for the residence time of the experiments with a defined flow rate of 0.36 mL/s and an initial tracer concentration of 0.3703 mg/mL is shown in Figure XI.

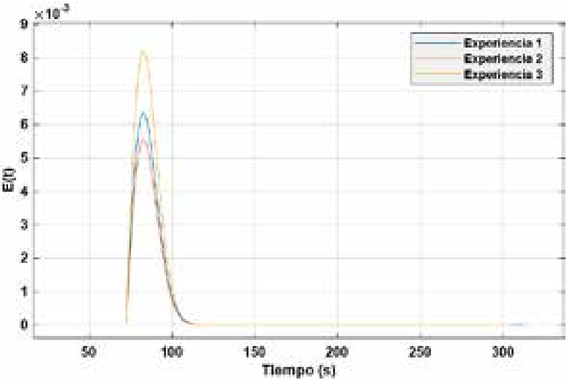

FIGURE XI

Weibull distribution for residence time with a flow rate of 0.36 mL/s and a tracer concentration of 0.3703 mg/mL.

TABLE III

Standard deviation, variance, and percentage error for a flow rate of 0.36 mL/s, varying concentrations.

| Flow rate 0.36 mL/s (20V) | | | | |
|---|---|---|---|---|
| Tracer concentration (mg/mL) | Residence time (s) | Standard deviation (s) | Variance ($s^2$) | Percentage error % |
| | 84.99 | 6.949 | 48.29 | 10.42 |
| 1.1109 | 84.99 | 6,949 | 48.29 | 10.42 |
| | 111.9 | 44.03 | 1938 | 17.93 |
| Average | 93.96 | 19.31 | 678.19 | 12.92 |
| | 108.6 | 6.949 | 48.29 | 14.45 |
| 0.3703 | 78.09 | 6,949 | 48.29 | 17.69 |
| | 85.59 | 6,949 | 48.29 | 9.788 |
| Average | 90.76 | 6,949 | 48.29 | 13,976 |

TABLE IV

Standard deviation, variance, and percentage error for a flow rate of 0.537 mL/s and a concentration of 1.1109 mg/mL.

| Flow rate 0.573 mL/s (22V) | | | | |
|---|---|---|---|---|
| Tracer concentration (mg/mL) | Residence time (s) | Standard deviation (s) | Variance ($s^2$) | Percentage error % |
| | 108 | 383 | 1467 | 23.72 |
| 1.1109 | 78.49 | 6,949 | 48.29 | 10.05 |
| | 91.27 | 39.6 | 1568 | 4.59 |
| Average | 92.59 | 143.18 | 1027.76 | 12.79 |

To determine the water flow rate of a 24 V Grothen pump, we worked within an optimal range where the flow rate was constant and the pump's power was not compromised by system overheating. It was observed that in the range between 16 V and 0.57 mL/s, the pump's performance was ideal for obtaining a correlation (R($^{(2)}$very close to 1, which is consistent with the behavior of a straight line. For the final experiment, it was decided to work with a flow rate between 0.36 mL/s and 0.57 mL/s, where the pump always operated efficiently without compromising the flow rate.

With regard to the dye calibration curve (Figure V), the voltage read by the brightness change detection system was plotted on the X-axis against the concentration of the solution on the Y-axis, in order to use the equation of the straight line obtained in that graph to calculate the output concentration read by the detection system in the experiment with the tracer.

Initially, eleven points were plotted, including the stock solution (10% m/V), nine serial dilutions, and water, representing the smallest voltage measured. The graph showed two behaviors: the higher concentration solutions followed a polynomial trend, while the lower concentration solutions followed a linear trend. It was decided to eliminate the three solutions with the highest concentration, as they were not necessary for the measurements of the light change detection system. Finally, a graph with eight points (seven dilutions and water) was obtained, called the dye calibration curve, which showed linear behavior with a correlation coefficient ($R^2$ ) of 0.9836, indicating good affinity with the experimental points.

Once the graph of concentration as a function of the voltage read by the light change detection system and the graph of flow rate as a function of voltage had been produced, the experiment with the tracer was carried out. A total of three experiments were carried out: the tracer with a concentration of 1.1109 mg/mL (solution A) and 0.36 mL/s for the flow rate, the tracer with a concentration of 1.1109 mg/mL (solution A) and 0.57 mL/s for the flow rate, and a tracer with a concentration of 0.3703 mg/mL (solution B) and a flow rate of 0.36 mL/s. The corresponding graphs were then produced, with the elapsed time plotted on the X-axis and the LDR sensor reading on the Y-axis.

Additionally, each experiment was performed and graphed in triplicate. For this reason, three curves can be seen in each graph. These curves show a difference between each other due to the lack of stability of the flow supplied by the pump, because despite maintaining the voltage when repeating each experiment three times, throughout the experimental work it was observed that the pump supplied a greater or lesser flow rate over time. It is considered that this causes the difference between the three curves in each graph, since the rest of the parameters were controllable and remained constant. This change in flow rate was present throughout each experiment despite waiting three minutes.

Prolonged use of the pump caused slight heating, which affected the repeatability of the experiment results. Heating decreases the efficiency of the pump, as part of the energy is converted into heat, reducing the flow rate supplied [17]. Temperature affects operational stability and the pressure generated, impacting the results and their repeatability, especially when performing triplicates of each experiment in a steady state.

The three experiments mentioned above: tracer with a concentration of 1.1109 mg/mL (solution A) and 0.36 mL/s for the flow rate, tracer with a concentration of 1.1109 mg/mL (solution A) and 0.57 mL/s for the flow rate, and tracer with a concentration of 0.3703 mg/mL (solution B) and 0.36 mL/s for the flow rate. They will be related in two different cases for analysis:

*Case 1:* Variable flow rate while maintaining concentration. For this experiment, concentration A (1.1109 mg/mL) was used for 1 mL of the tracer, and the flow rate was varied by changing the voltage from 0.36 mL/s to 0.57 mL/s. Figure VI shows the behavior of the tracer for 0.36 mL/s, while Figure VIII shows the behavior of the same tracer, but at 0.57 mL/s. Then, in Figures VII and IX, respectively, the Weibull distribution is performed to model the data obtained in each experiment.

*Case 2:* Variable concentration while maintaining flow rate. For this experiment, a fixed voltage of 0.36 mL/s was used for the flow rate, and the tracer concentration was varied, using A (1.1109 mg/mL) on one occasion and B (0.3703 mg/mL) on another occasion. The higher concentration (A: 1.1109 mg/mL) with 0.36 mL/s for the flow rate is shown in Figure VI, and the lower concentration (B: 0.3703 mg/mL), also with 0.36 mL/s for the flow rate, is shown in Figure 12. Subsequently, their Weibull distribution is observed in Figures VII and XI, respectively.

Starting with case 1, in Figure VI (concentration graph A: 1.1109 mg/mL with 0.36 mL/s for the flow rate), Table III shows that the residence time for the three repetitions is on average 93.96 seconds, while for Figure VIII (concentration A: 1.1109 mg/mL with 0.57 mL/s for the flow rate), Table IV shows that the average residence time is 92.56 seconds. In other words, as the flow rate through the burette increases, the residence time of the tracer decreases. This coincides with what is theoretically expected, since the fluid passes more quickly through the reactor, reducing the time that each reactant molecule remains in the system and thus decreasing the residence time [18].

In case 2, it was observed that the average residence time for a concentration of 1.1109 mg/mL is 93.96 seconds, while for a concentration of 0.3703 mg/mL it is 90.76 seconds. This indicates that the residence time is longer with higher concentrations and shorter with lower concentrations, fulfilling a directly proportional relationship. This does not coincide with what is theoretically expected, since the residence time does not depend on the tracer concentration [11]. These discrepancies observed between the theoretical and experimental results may be related to errors in the experiment, such as the lack of a constant flow supplied by the pump and its overheating. However, it can be seen that the difference between the two times is not very large.

In Figure VI, it can be seen that the residence time for the three repetitions is between 175 and 225 seconds. However, Table 3 shows an average residence time of 93.96 seconds calculated using the Weibull distribution, which fits the data by modeling accelerated growth followed by a long tail. This distribution was chosen because of its similarity to the experimental data. Comparing this residence time with the spatial time (Tao) yields an error of 12.92%, indicating that the reactor behaves close to ideal. The effects of diffusion and friction on the walls are low due to the larger relative surface area in contact with the fluid and the laminar flow, which reduces resistance to fluid movement.

In the three experiments carried out, there is a difference between the resistance time displayed directly on the graph (the moment when the reading of the light change detection system remains constant) and that calculated using the Weibull distribution. As mentioned above, this may occur because the fit is not perfect for the curve, although it is a very good approximation, and that is without considering the visual error when reading the graph and defining the time at which it remains constant.

Finally, the standard deviation and variance are also not very significant for the three experiments (detailed in Tables 3 and 4). for the standard deviation, an average of 19.31 sec, 6.949, and 143.18 sec was obtained, respectively. The only high value is the last one, and this was due to one of the repetitions in which the pump was malfunctioning and, therefore, unreliable results were obtained for that repetition, affecting the standard deviation of that last experiment. For the variance, an average of 678.19$s^2$ , 48.29$s^2$ , and 1027.76$s^2$ was obtained, respectively. The two high results are also due to a measurement in which the pump did not maintain a constant flow rate, making the repeatability of the experiments difficult.

## Conclusions

This study has demonstrated the feasibility of using a laboratory-scale piston flow reactor (PFR) to characterize residence time distribution (RTD) in non-ideal systems.

The implementation of a real-time data acquisition system, based on an Arduino UNO and an application developed in MATLAB App Designer, allowed for accurate and reliable measurements.

The use of the Weibull distribution to model the non-ideal behavior of the reactor was validated, observing that the increase in flow rate from 0.36 mL/s to 0.57 mL/s reduced the average residence time.

The calibration curves for the flow rate and the light change detection system showed a high degree of reliability ($R^2 = 0.9836$ and $R^2 = 0.9837$, respectively), although limitations related to flow stability due to pump heating were identified, highlighting the need to control operational factors to ensure system stability and repeatability.

The experimental design and the application developed provide a valuable educational platform for the study of reactive systems, allowing students to replicate the experiment and analyze data in real time.

This work not only contributes to the understanding of RTD phenomena in non-ideal reactors, but also highlights the usefulness of modern tools in chemical engineering education.

Future research could focus on improving the stability of the system and exploring other reactor configurations to broaden the educational scope of this work, thus consolidating its relevance in the training of chemical engineers.

## References

[1] Rodgers, T. (2013). *Chemical Reaction Engineering*. https://personalpages.manchester.ac.uk/staff/tom.rodgers/documents/CRE_Notes.pdf

[2] López, I., & Borzacconi, L. (2009). *Introduction to Reactor Design*. https://boletines.exportemos.pe/recursos/boletin/RESUMEN%20CINETICA.pdf

[3] Levenspiel O. (1999) *Chemical Reaction Engineering* https://drive.google.com/file/d/1eqjAs4cfjGCd9SsCUuMKZvJ2Qr_uZDxM/view

[4] Fogler, S. (2006). *Models for nonideal reactors* (4th ed.). Pearson Education, Inc. https://public.websites.umich.edu/~essen/html/byconcept/cdchap/14chap/ECRE_CD-CH14.pdf

[5] Liu, Z. (2014). *Physical principles of environmental systems*. https://bae.engg.ksu.edu/~zifeiliu/files/fac_zifeiliu/Zifeiliu/BAE820_16%20Type%20of%20reactors.pdf

[6] Huang, P. Y., &amp; Feng, J. (1995). Wall effects on the flow of viscoelastic fluids around a circular cylinder. *Science Direct*, *60*(2), https://www.sciencedirect.com/science/article/abs/pii/0377025795013942.

[7] Klewicki, J., Saric, W., Marusic, I., & Eaton, J. (2007). Wall-Bounded flows. In *Springer eBooks* (pp. 871-907). https://doi.org/10.1007/978-3-540-30299-5_12

[8] Chalmers, H., Fang, X., Addai, S., & Tachie, M. F. (2022). The effects of wall roughness on the flow dynamics behind a near-wall square cylinder. *Experiments In Fluids*, *63*(8). https://doi.org/10.1007/s00348-022-03472-z

[9] *Dispersion in flow reactors*. (n.d.). Vapourtec. https://www.vapourtec.com/wp-content/uploads/2015/10/Vapourtec_Dispersion.pdf

[10] Dudokovic, M. P., & Felder, R. M. (n.d.). *Mixing effects in chemical reactors*. https://classes.engineering.wustl.edu/eece503/Lecture_Notes/Module_3.pdf

[11] Fogler, H. S. (2006). Engineering elements of chemical reactions (4th ed.). Pearson Educación de México. ISBN: 978-970-26-1198-1.

[12] Román-Raya, J., Ruiz-García, I., Escobedo, P., Palma, A. J., Guirado, D., & Carvajal, M. A. (2020). Light-Dependent Resistors as Dosimetric Sensors in Radiotherapy. *Sensors*, *20*(6), 1568. https://doi.org/10.3390/s20061568

[13] Deetman, A., Bos, D., Blaakmeer, J., Salet, T., &amp; Lucas, S. (2024). An in-line dye tracer experiment to measure the residence time in continuous concrete processing. *Materials And Structures*, *57*(5). https://doi.org/10.1617/s11527-024-02378-y

[14] Jabar, M. (2022). *PROPERTIES OF LIGHT*. Retrieved November 27, 2024, from https://uomustansiriyah.edu.iq/media/lectures/6/6_2022_10_14!01_14_27_PM.pdf

[15] Diaz NA, Bárcena Ruiz A, Fernández Reyes E, et al. Spectrophotometry: absorption spectra and colorimetric quantification of biomolecules. Department of Biochemistry and Molecular Biology, Rabanales University Campus. https://www.uco.es/dptos/bioquimica-biol-mol/pdfs/08_ESPECTROFOTOMETRIA.pdf.

[16] Porral, Edgardo &amp; Battaglia, Gerardo. (2022). ELECTRONIC PHYSICS Introduction to Quantum Physics. https://www.researchgate.net/publication/366433259_FISICA_ELECTRONICA_Introduccion_a_la_Fisica_Cuantica

[17] Calderón, G., &amp; Contreras, R. (2003). *STUDY OF CAVITATION IN CENTRIFUGAL PUMPS*. https://repositorio.utb.edu.co/bitstream/handle/20.500.12585/3613/0024437.pdf?sequence=1

[18] Guo, X., Fan, Y., & Luo, L. (2018). Residence Time distribution on flow Characterisation of multichannel systems: modeling and experimentation. *Science Direct, 99,* https://www.sciencedirect.com/science/article/abs/pii/S089417771830877X?via%3Dihub

[19] Carrasco, J., Ortega, E., &amp; Cordeiro, G. (2008). A generalized modified Weibull distribution for lifetime modeling. *Science Direct*, *53*(2). https://www.sciencedirect.com/science/article/abs/pii/S0167947308004192

[20] Díaz, N., Bárcena, J. A., Galván, A., Peinado, J., Toribio, F., &amp; Túnez, I. (n.d.). *Spectrophotometry: absorption spectra and colorimetric quantification of biomolecules*. https://www.uco.es/dptos/bioquimica-biol-mol/pdfs/08_ESPECTROFOTOMETRIA.pdf

[21] *The photoelectric effect in an LDR Objective*. (2019, April 2). studylib.es. https://studylib.es/doc/7162424/el-efecto-fotoel%C3%A9ctrico-en-un-ldr-objetivo

[22] Thibaut. (2022, September 30). *Beer-Lambert law - IMA*. IMA. https://imamagnets.com/blog/ley-de-beer-lambert/

[22] Escalona, L. (2007). Experimental Determination of the Distribution of Residence Times in an Agitated Pulp Tank. https://www.metsolver.com/Papers/dt1.pdf